Photonic Network Communications
https://doi.org/10.1007/s11107-019-00873-9

ORIGINAL PAPER

Assessment of novel regenerator assignment strategies in dynamic translucent elastic optical networks

Emerson F. da Silva[1] · Raul C. Almeida Jr.[3] · Helder A. Pereira[2] · Daniel A. R. Chaves[1]

Received: 7 June 2019 / Accepted: 5 November 2019

Abstract
The problem of regenerator assignment (RA) in translucent optical networks consists in segmenting a lightpath into several transparent segments, each of which linked by 3 R regenerators. In this article, we present two heuristics and compare their effectiveness with an exhaustive method to solve the RA problem in translucent elastic optical networks under dynamic traffic. The exhaustive method is capable of finding solutions that are able to minimize, simultaneously, the number of regenerators and frequency slots used in a given route. It is assumed 3 R regenerators, which are capable to perform both modulation format and spectrum conversion. In our simulations, we consider the amplified spontaneous emission noise generated by optical amplifiers as physical impairment. Two practical mesh topologies have been analyzed in terms of call request blocking probability. The results show that the presented heuristics are able to find solutions that provide very similar performance to those found by utilizing the best solutions of the exhaustive method.

Keywords Elastic optical network · Physical impairment · Regenerator assignment · Regenerator placement · Signal-to-noise ratio

1 Introduction

Wavelength division multiplexing (WDM) networks are able to provide large transmission capacity. However, when network clients present heterogeneous traffic demands, inflexibility in the bandwidth usage of wavelengths may lead to a non-optimized use of the available frequency spectrum. In order to overcome this limitation, it is possible to improve the optical frequency spectrum usage by dividing it in slices narrower than in WDM, known as frequency slots. This approach is known in the literature as elastic optical networks (EON) [1–3].

Depending on in which nodes regeneration resources are installed/used, optical networks can be classified as: (1) opaque, (2) transparent and (3) translucent [4, 5].

In opaque networks, the optical signal is converted into the electrical domain in each network node along its path. After this conversion, the signal is re-amplified, re-shaped and re-timed (3 R regeneration). Then, the electrical signal is converted back into the optical domain. The implementation cost of this kind of network becomes very high if several channels must be implemented. However, here we have the advantage that the propagating optical signal does not accumulate excessive physical impairments imposed by the optical devices and optical fibers because it is regenerated at each node along the path.

The most forcible proposal to reduce the high cost of opaque networks is to completely eliminate O/E/O conversion in the network. This proposal is named as transparent network. Although the cost of the network is substantially reduced, such alternative may result in excessively high physical impairments accumulation by optical signals that traverse several hops, which may eventually prevent the establishment of exigent low bit-error-rate call requests or force the use of low-efficiency modulation formats.

✉ Daniel A. R. Chaves
darc@ecomp.poli.br

Raul C. Almeida Jr.
ralmeida.ufpe@gmail.com

[1] Polytechnic School of Pernambuco, University of Pernambuco, Recife, Pernambuco, Brazil

[2] Electrical Engineering Department, Electrical Engineering and Informatics Center, Federal University of Campina Grande, Campina Grande, Paraiba, Brazil

[3] Photonics Group, Department of Electronics and Systems, Center of Technology and Geosciences, Federal University of Pernambuco, Recife, Pernambuco, Brazil

Published online: 10 December 2019

The third possibility, known in the literature as translucent networks, tries to combine the advantages of both opaque and transparent optical networks. In translucent optical networks, a certain amount of 3 R regeneration resources shall be strategically distributed in the network. An usual strategy aims to install as few as possible O/E/O devices (regeneration resources) in the network [6] and perform optical signal regeneration only when it is required. This enables that both the quality of transmission (QoT) and the network CapEx be kept at acceptable levels.

In translucent EONs, the choice of which nodes will be either equipped with 3 Rs (translucent nodes) or not (transparent nodes), and how/when to use the regeneration resources in their translucent nodes are important research topics. The former is known as regenerator placement (RP) and the latter as regenerator assignment (RA) [6–8]. The RP consists in deciding in which network nodes 3 R regeneration resources will be installed as well as their amount per node. Thus, 3 R regenerator placement decisions represent a design decision and usually take place prior to the network operation stage. Usually, the RP decisions affect the network in terms of performance, capital expenditure and energy consumption [9, 10].

In a broader sense, the objective of an RA algorithm is to determine in which nodes of the lightpath the optical signal should, or should not, be regenerated. Basically, the RA algorithm takes as input a route and divides it into a set of successive transparent segments (TS), which are linked by regeneration resources. Suppose a route composed by h hops. The number of transparent segments in the route may vary from 1, if no 3 R regeneration resource is used in the route, to h, if 3 R regeneration resource is used in all intermediary nodes of the route.

In WDM networks, the use of regenerators can promote two improvements in network performance: bring the optical signal-to-noise ratio (OSNR) of the optical signals back to high values, thus increasing the signal's maximum reach; and permit wavelength conversion, which results in flexibilization on the wavelength continuity constraint and a consequent increase on the number of attended calls [6]. In addition to these benefits described, the use of regeneration in EONs can also provide spectrum saving. This occurs because different modulation formats require different spectrum capacity and, differently from WDM, EONs can provide lightpaths with variant bandwidth. Therefore, now, it is possible to establish a lightpath with few transparent segments, use few regenerators, but a large number of slots due to the necessity of using modulation formats with low spectral efficiency; or segment the optical path into additional transparent segments, use modulation formats with higher spectral efficiency and reduce the network slot usage [7]. In other words, in EONs, there is a trade-off between the number of regenerators and slots used to attend a lightpath. Although not commercially available, the modulation format and spectrum conversions may be performed all-optically instead of using electronic 3R [11].

In networks under dynamic traffic, the RA algorithm should be implemented in the control plane (CP) of the network. In such case, the CP performs the decision of how to use the installed regenerators in a per demand basis (i.e., request by request) [7, 8]. In networks under static traffic, on the other hand, the problems of regeneration placement and regeneration assignment are jointly performed in a single phase. This is because all the requests are known beforehand and regeneration resources are specifically installed to support a request where it is necessary.

This paper provides a more detailed description and a more extensive performance analysis of two novel heuristics used to perform regenerator assignment in translucent EONs, introduced in [7]. Moreover, we also compare the proposed heuristics against an exhaustive method to perform regenerator assignment in translucent EONs. The novelties of the paper are: (1) Comparison of the heuristics methods against the exhaustive approach to solve RA problem which considers the simultaneous minimization of the number of regenerators and frequency slots used in a route; (2) the analysis of non-optimality of the heuristics; (3) the time complexity analysis of the heuristics; (4) the analysis of the heuristics under several different network scenarios, such as: different sets of available modulation formats, offered load, number of slots and regenerators, as well as different values for launch powers and amplifier noise figures; and (5) how one can compare them with the optimal fixed solution provided by the exhaustive approach. The extended analysis provided in this paper radically improves the assessment of the heuristics by demonstrating their effectiveness in finding almost optimal solutions in typical network topologies.

The paper is organized as follows. In Sect. 2, we present a literature review about regenerator assignment problem applied to EONs. In Sect. 3, we describe our RA algorithms. In Sect. 4, we describe in details the simulation setup and the network scenarios used in our simulations. In Sect. 5, we present and discuss the obtained results and, finally, in Sect. 6, we present the conclusions.

2 Literature review

In this paper, we assume the scenario of networks under dynamic traffic. As pointed out in Sect. 1, there are very few works in the literature dealing with RA in dynamic scenarios. Although the RA problem under dynamic and static traffics are different from each other in the point of view of network planning and control plane implementation, there are some optimization characteristics that are similar in both scenarios. For that reason, we decided to present a literature review of RA proposals in both dynamic and static scenarios. Although the RP and RA problems are jointly executed under static traffic, we refer to the problem as RA, either we are referring to static or dynamic traffic. Note that the typical communication services supported by the optical backbones require a path computation time smaller than a certain limit, which vary from 10 to 100 ms depending on the considered service [12].

2.1 Literature about RA under static traffic

An usual strategy to perform RA in networks under static traffic is to perform the route segmentation, i.e., regenerator sites selection, by minimizing either an weighted sum of number of regenerators and total number of frequency slots used in the route [13–17] or simply by minimizing the frequency spectrum usage regardless the amount of regenerators deployed [18–20]. In most of these works, all available choices for route segmentation are considered.

Yamazaki et al. [21] propose to perform the route segmentation by carrying the signal as far as possible from the source node. However, the nodes allowed to deploy regenerators are determined by a firefly optimization algorithm which aims to minimize the total number of regenerators installed in the network.

Finochietto and Bianco [22] propose three strategies to perform RA: (1) the reactive provisioning strategy, which gives priority to allocate demands using an end-to-end transparent lightpath and, just when no transparent path is found, an opaque path is searched; (2) the conservative provisioning strategy, which always establishes opaque lightpaths, i.e., regenerates the signal at each intermediary node; and (3) the proactive provisioning, which switches between the use of the former two strategies based on a frequency spectrum congestion level threshold.

Yan et al. [23] proposed an RA strategy based on the probability of using a regenerator in a given node, considering a greenfield scenario, in which all source–destinations pair connections are known in advance but their transmission rates vary along the time.

2.2 Literature about RA under dynamic traffic

Yang and Kuipers [24] propose an RA strategy performed in two steps: firstly, alongside with the RSA algorithm, it is assumed that each node with available regeneration resource will regenerate the signal. Then, another algorithm selects only the nodes that truly need regenerators. This algorithm tries to carry the optical signal as far as possible using the available modulation format with higher noise tolerance without considering modulation format conversion. They modify their algorithm to cope with modulation format conversion by introducing an auxiliary multi-layer graph, in which each layer represents a modulation format.

In [7], we propose two heuristics to perform RA in EONs. These proposed algorithms were used in [8] and [25] to carry out performance and cost analysis in translucent EONs.

Guo et al. [26] perform their RA algorithm by finding the minimum number of regeneration resources (r) required for a given route based only in the route length and transmission reach. Among the solutions with the minimum number of regenerators, it selects the one that minimizes a cost function that takes into account the consumed frequency spectrum resources.

Walkowiak et al. [27] proposed an RA which works alongside with the routing process. Their algorithm considers several possibilities of routing segmentation on the candidate routes and performs the selection of the route–segmentation pair using a cost function that takes into account the number of slots and regenerators used by the candidate.

It is worth to point out an intrinsic difficulty to perform regenerator assignment in translucent EONs: if one tries to find solutions that reduce the number of used regenerators, this leads to a high spectral usage in the network. On the other hand, if one tries to find solutions that mitigate the number of used frequency slots, this leads to a high regenerators usage. As shown in this section, there are strategies that try to reduce either the spectral usage or the number of deployed regenerators, but not both simultaneously. The exhaustive RA algorithm used in this paper presents this latter capability.

3 Regenerator assignment algorithms

In this section, we describe two distinct resource-saving heuristics to perform regenerator assignment in translucent EONs, compare them with an exhaustive method, and provide a detailed discussion about the heuristics non-optimality and time complexity. The first heuristics (Sect. 3.1) gives preference to select the modulation format with the highest possible spectral efficiency, which implies in saving frequency spectrum at the cost of establishing short transparent segments and therefore using a large amount of regenerators. Since it tries to save frequency spectrum, it is named as first narrowest spectrum (FNS-RA) [7, 8]. The second heuristics (Sect. 3.2) aims to transmit the optical signal as far as possible by avoiding the use of regeneration resources the most it can. It is named as first longest reach (FLR-RA) [7, 8]. The exhaustive method (Sect. 3.3) uses the concept of dominance to find optimal solutions in terms of the number of regenerators and frequency slots used by each established connection, which can be used as benchmark for verifying the FLR-RA and FNS-RA heuristics effectiveness.

All RAs described in this section are allowed to use regenerators to perform: (1) optical signal regeneration, in order to solve the lack of QoT; (2) frequency spectrum conversion, in order to solve the lack of frequency slots continuity and contiguity and (3) modulation format conversion to select the most suitable modulation format (MF) to each transparent segment (TS).

3.1 First narrowest spectrum regenerator assignment

FNS-RA is a greedy algorithm that aims in saving network spectrum. This is performed by trying to establish transparent segments with the most efficient modulation format, which requires the minimum amount of spectrum, regardless the number of required regenerators for that.

Let $P = (n_0, n_1, \ldots, n_x, \ldots, n_{N-1})$ be the route chosen to establish the request. We assume that the modulation formats are indexed as $m = 1, 2, \ldots, M$ and, the lowest is the value of m, the highest is the spectral efficiency of the MF.

FNS-RA starts by considering the most spectrally efficient modulation format (i.e., $m = 1$). Then, it searches for a transparent segment from the source node n_0 to the farthest possible node n_x with available regeneration capability, so that the transparent segment from n_0 to n_x attends QoT criterion as well as frequency spectrum availability. If a transparent segment is found, it is selected and the node n_x becomes the new source node and the process is restarted using n_x as the source node. On the other hand, if a transparent segment cannot be established with the most efficient modulation format, the algorithm searches for the shortest transparent segment that can be established with one of the other modulation formats ($m = 2, 3, \ldots, M$, in this order) that attends the QoT criterion as well as spectrum contiguity and continuity.

The reason of searching for the shortest transparent segment instead of the longest one is to avoid using, through several links of the network that would compose a long transparent segment, an unnecessary amount of spectrum required by modulation formats with low spectral efficiency. Establishing short transparent segments when the most efficient MF cannot be used gives more chance for FNS-RA to assign the most efficient MF along the subsequent transparent segments, which shall end up saving network spectrum resource. As a consequence, FNS-RA may end up using a large number of regenerators for a given route.

It is expected that FNS-RA presents low call request blocking probability in network scenarios with a large number of regenerators installed or a low amount of available frequency slots.

Algorithm 1 Pseudo code for FNS-RA and FLR-RA heuristics

Require: Bit rate (b) and Route ($n_0, n_1, n_x, ..., n_{N-1}$)

1: $s \leftarrow -1$ ▷ route index of the current source node
2: $x \leftarrow 0$ ▷ route index of the current destination node
3: $r \leftarrow 1$; ▷ route index of the last feasible regeneration point
4: $m \leftarrow 1$; ▷ current modulation format index
5: **while** ($s \leq N-1$) **do** ▷ loop for testing TS source node
6: $s \leftarrow s+1$
7: $segmenting \leftarrow true$ ▷ true while current TS is not yet defined
8: **while** ($x \leq N-1$ **and** $segmenting = true$) **do** ▷ loop for testing TS destination node
9: $x \leftarrow x+1$
10: **if** (isThereFreeRegenAt(n_x,b) or ($n_x = n_{N-1}$)) **then** ▷ n_x has free regenerators or it is the destination node
11: **if** (isThereSpectumAndOSNR(n_s,n_x,m)) **then** ▷ check if the transparent segment (n_s, n_x) can be established
12: **if** ($n_x = n_{N-1}$) **then** ▷ check if destination node is reached
13: store the TS from n_s to n_x; ▷ store the last TS
14: perform MF and SA for all stored TS; ▷ establishes in the network all stored TS
15: finish the algorithm.
16: **else** ▷ destination not reached yet
17: **if** ($m \neq 1$) **then** ▷ current MF is not the best one
18: store the TS from n_s to n_x.
19: $s \leftarrow x-1$; ▷ update the current TS source node index
20: $r \leftarrow x+1$; ▷ update node index of feasible regeneration point
21: $segmenting \leftarrow false$; ▷ current TS is defined
22: $m \leftarrow 1$; ▷ switch back to the best MF
23: **else** ▷ best MF (m=1) is under use
24: $r \leftarrow x$; ▷ updates the feasible regeneration node index
25: **else** ▷ current TS under test is not feasible
26: **if** ($r \neq x$) **then**
27: Store the TS from n_s to n_r;
28: $s \leftarrow r-1$; ▷ update the current TS source node index
29: $x \leftarrow r$; ▷ update the current TS dest. node index
30: $r \leftarrow r+1$; ▷ update node index of feasible regeneration point
31: $segmenting \leftarrow false$; ▷ current TS is defined
32: **else** ▷ current TS is not feasible using m MF
33: $x \leftarrow x-1$; ▷ update TS dest. node index
34: $m \leftarrow m+1$; ▷ change MF and try again
35: **if** ($m > M$) **then** ▷ all MF were unsuccessfully tried?
36: Block the current call request;
37: finish the algorithm;

The pseudocode for the FNS-RA is presented in Algorithm 1. There are two functions used in Algorithm 1: (1) isThereFreeRegenAt(n_x,b), which is a boolean function that returns true if there are available regenerators at node n_x to regenerate bit streams with a respective transmission bit rate (b), and false otherwise (refer to Sect. 4.3 for further details on relationship between the number of required regenerators and bit rates); and (2) isThereSpectumAndOSNR(n_s,n_x,m), which is also a boolean function that returns true if the modulation format m may be assigned to the transparent segment between nodes n_s and n_x, in terms of both OSNR and available frequency spectrum, and false otherwise.

3.2 First longest reach regenerator assignment

FLR-RA is a greedy algorithm that aims to transmit the optical signal as far as possible without needing regeneration. In other words, FLR-RA tries to use the smallest possible number of regenerators to implement a given route.

Let again $P = (n_0, n_1, \ldots, n_x, \ldots, n_{N-1})$ be a route with N nodes. The FLR-RA starts by trying to establish a transparent segment from the source node n_0 to the farthest possible node n_x with available regeneration capability, so that the transparent segment from n_0 to n_x attends QoT criterion as well as frequency spectrum availability (i.e., contiguity and continuity). Therefore, it is possible (and usually is) that a not very efficient modulation format is used in order to attend the search for the farthest possible regeneration point. If there is such node n_x, the optical signal is regenerated at node n_x and a transparent segment from n_0 to n_x is established. Then, n_x becomes the new source node and the process restarts until the destination node (n_{N-1}) is reached.

The detailed operation of FLR-RA can be described by doing the following modifications in Algorithm 1: (1) removal of the highlighted lines in Algorithm 1 and (2) replacement of the function isThereFreeRegenAt(n_x,b,m) by

the function isThereFreeRegenAt(n_x,b) (line 11). The new function is also a boolean function that returns true if there is, at least, one modulation format capable of being assigned to the transparent segment between nodes n_s and n_x, in terms of both optical signal-to-noise ratio (OSNR) and available frequency spectrum; and false otherwise.

Notice that the FLR-RA concept aims to avoid using unnecessary regeneration resources whenever possible. Therefore, it is expected that the FLR-RA presents good performance in network scenarios in which there are few available regenerators in each node or there is sufficiently large available frequency spectrum.

Observe that, for both FNS-RA and FLR-RA, we have assumed in line 14 of Algorithm 1 that the most spectrally efficient modulation format that meets both the QoT and spectral availability is always assigned to each TS.

3.3 Exhaustive regenerator assignment

In this paper, we used as a comparison purpose an exhaustive method (E-RA) for regeneration assignment similar to the one proposed in [28]. For a given route P, the E-RA identifies all nodes with available regeneration resources and tests all possible RA solutions for P that simultaneously attend the QoT criterion and frequency spectrum continuity and contiguity. Let F be the set with all these solutions. For each solution i ($i \in F$), the algorithm calculates the number of regeneration points (r_i) used in it, as well as the total number of frequency slots (f_i) used along all physical links of the transparent segments of the solution. Then, the dominance rule is applied to the set F and the dominated solutions are removed from F. A solution i belonging to the set F is called dominated if exists at least one solution j that belongs to F such that either $r_j \leq r_i$ and $f_j < f_i$ or $r_j < r_i$ and $f_j \leq f_i$ [29].

Note that the method E-RA provides a set of possible RA solutions instead of a single solution as both heuristics FLR-RA and FNS-RA do. Therefore, in order to compare the E-RA algorithm with FLR-RA and FNS-RA heuristics, we have defined two selection policies to choose one single solution from the set F: (1) Er-RA, which selects from F the solution i with the minimum value of r_i; and (2) Es-RA, which selects from F the solution with the minimum value of f_i. Since E-RA tries all possible solutions, Er-RA and Es-RA always find the solution with either the minimum number of regenerators or the minimum number of frequency slots, respectively, which are optimal solutions if the chosen metric aims in reducing either the number of regenerators or frequency slots. Thus, one may compare in a fair basis the results provided by Er-RA with the results provided by FLR-RA, as well as the results provided by Es-RA with the results provided by FNS-RA.

3.4 Examples of FLR-RA and FNS-RA non-optimality

Both FLR-RA and FNS-RA are greedy algorithms in the sensing of heuristically searching for minimizing the proposed metric. Therefore, any of them may end up not returning the best solution in terms of number of required frequency slots from the FLR-RA (which focus on minimizing the number of used regenerators) and number of required regenerators from the FNS-RA (which focus on minimizing the number of used frequency slots). In this section, we provide some cases in which the non-optimally of the proposed RA heuristics can be observed.

In order to present an analysis regarding the non-optimality of the FLR-RA and FNS-RA heuristics, let us suppose, for simplicity of analysis, the case of a network where all links are formed by the same number of spans (s) and the spans have the same length. Suppose that the transponders and regenerators are capable of generating $M = 3$ modulation formats ($m = 1, 2, 3$) and that the m-th MF may transmit the optical signal along h_m spans, where again we assume that the MFs are indexed so that the lower is m, the higher is the spectral efficiency of the modulation format. Therefore, for $m = 1, 2, 3$, the optical signal may be transmitted, at most, for h_1, h_2 and h_3 spans by using bw_1, bw_2 and bw_3 frequency slots, respectively, where $h_1 \leq h_2 \leq h_3$ and $bw_1 \leq bw_2 \leq bw_3$. Moreover, suppose the scenario S in which the optical signal can reach with enough QoT: 3 hops using $m = 3$ ($h_3 > 3s$) but cannot reach 4 hops ($h_3 < 4s$); 2 hops using $m = 2$ ($h_2 > 2s$) but cannot reach 3 hops ($h_2 < 3s$); and the signal cannot reach 1 hop using $m = 1$ ($h_1 < s$).

As discussed in Sect. 3.2, the FLR-RA aims at finding a solution using as few as possible regenerators in a given route. The FLR-RA non-optimality may occur whenever it uses more frequency slots than required for the solution with minimum number of regenerators. Assuming the scenario S and a route composed by 4 links, the solution given by FLR-RA uses $m = 3$ in the first 3 hops and $m = 2$ in the last hop. This solution uses one regeneration point (at the end of the third hop) and a total of $3bw_3 + 1bw_2$ frequency slots. However, there is a solution that also performs regeneration in a single point, but uses less frequency slots if $bw_2 < bw_3$, which is: $m = 2$ in the first 2 hops and $m = 2$ in the last 2 hops, using a total of $4bw_2$ frequency slots. Notice that the second solution uses fewer frequency slots with the same number of regeneration points (minimum possible).

For the sake of comparison with the exhaustive method Er-RA, note that the second solution (with $r_2 = 1$ and $f_2 = 4bw_2$) is the one chosen by the Er-RA instead of the solution chosen by the FLR-RA (with $r_1 = 1$ and $f_1 = 3bw_3 + 1bw_2$). In this example, the first solution is eliminated from the final solution given by the exhaustive

method because the second solution dominates the first since $r_2 = r_1$, but $f_2 < f_1$.

A similar case may occur to the FNS-RA, but now the optimality is lost due to an unnecessary number of regenerators returned by its solution. Assuming again the scenario *S*, but now a route composed by 2 links, the solution provided by the FNS-RA uses $m = 2$ at both links, but with a regeneration point in the middle of the route. Clearly, there is a better solution which uses $m = 2$ in both links and does not use regenerators at the middle of the route.

Again, for the sake of comparison, Es-RA is able to find the solution with a smaller number of regenerators since the solution provided by FNS-RA is discarded by Es-RA due to the dominance rule.

Assuming a route in which all links have the same number of spans and all inequalities present in scenario *S* are simultaneously satisfied for that route, the number *s* of spans per link which necessarily leads to non-optimal solutions of both FLR-RA and FNS-RA heuristics is given by:

$$\max\left(\frac{h_3}{4}, \frac{h_2}{3}, h_1\right) < s < \min\left(\frac{h_3}{3}, \frac{h_2}{2}\right), \tag{1}$$

which is obtained by simultaneously satisfying all the inequalities stated for the number of spans (s) in scenario *S*.

3.5 Analysis of the algorithms time complexity

In order to investigate the time complexity of the investigated algorithms, let M be the number of available modulation formats and $\pi = (n_0, n_1, \ldots, n_x, \ldots, n_{N-1})$ be the route selected to establish the request. The nodes represented in π are only the ones with available regeneration capability in the selected route.

We are considering that the most time-consuming part of the algorithms is the evaluation of both OSNR and frequency spectrum continuity and contiguity for a given modulation format and transparent segment, henceforth, named as transparent segment check (TS-Check). For this reason, the algorithms' time complexity has been inferred as the number of times the TS-Check is performed. Note that the RA algorithm segments the route into k transparent segments (TS) each of one is x_k hops long and requires t_k TS-Checks evaluations.

Let us start by the time complexity evaluation of FLR-RA. The FLR-RA successively tests for each node n_x, along the route π, if the transparent segment ranging from the current source node n_s to the node n_x can be established in terms of both OSNR and spectrum continuity/contiguity (TS-Check). Eventually, the TS-Check fails in the node n_x and the regeneration should be performed in the previous node n_{x-1}. By starting the segmentation from the source node of π, suppose that, during the establishment of the first transparent segment the first TS-Check to fail occurs after $x_1 + 1$ hops from the source node, i.e., in the node n_{x_1+1} (i.e., the transparent segment from n_0 to n_{x_1+1}). It means that the signal should be regenerated in the node n_{x_1}. Consequentially, for this first transparent segment it is required, at most, t_1 ($t_1 = M(x_1 + 1)$) TS-Checks (one check for each M available modulation formats in each tested TS). Then, the node n_{x_1} becomes the new source node ($n_s = n_{x_1}$), and

part of the π not yet segmented is $|\overline{\pi_1}| = N - 1 - (x_1)$ hops long (the route ranging from n_{x_1} to n_{N-1}). Similarly, if the second transparent segment is x_2 hops long it ends in node $n_{x_1+x_2}$ and it is required for its determination, at most $t_2 = M(x_2 + 1)$ TS-Checks. The part of the π not yet segmented is $|\overline{\pi_2}| = N - 1 - (x_1) - (x_2)$ hops long. After the definition of k transparent segments, the remaining part of the π not segmented yet is $|\overline{\pi_k}| = N - 1 - \sum_{i=1}^{k}(x_i)$ hops long. Note that when the destination node is reached, necessarily, $|\overline{\pi_k}| = 0$ and $\sum_{i=1}^{k} t_i$ is the number of TS-Checks required, at most, during the entire route segmentation. Since $\sum_{i=1}^{k} t_i = \sum_{i=1}^{k}\{M(x_i + 1)\}$ one can write $\sum_{i=1}^{k} t_i = M\{k + \sum_{i=1}^{k}(x_i)\}$. As the destination node (n_{N-1}) is reached $|\overline{\pi_k}| = 0$ and, for this reason, $\sum_{i=1}^{k} x_i = N - 1$. By replacing the sum of x_i for the sum of t_i we can write $\sum_{i=1}^{k} t_i = M\{k + (N - 1)\}$. Since k is the number of transparent segments found by the FLR-RA, its maximum value is $N - 1$. Then, the maximum value for $\sum_{i=1}^{k} t_i$ is $M(2N - 2)$.

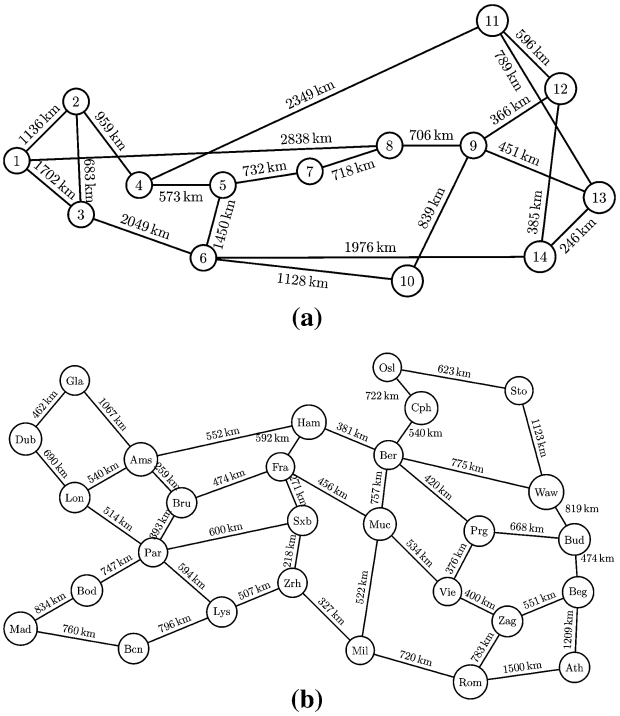

Fig. 1 Network physical topologies used in our simulations: **a** Topology 1 (NSFNet) and **b** Topology 2 (European), with distances in km

Therefore, the FLR-RA needs, at most, $M(2N-2)$ TS-Checks evaluations which leads to a $\mathcal{O}(M \cdot N)$ time complexity for FLR-RA.

The time complexity of FNS-RA algorithm can be evaluated similarly. The difference is, whereas the FLR-RA always tries to establish the longest TS possible, the FNS-RA establishes the longest TS possible only for the best MF (in terms of spectral efficiency). The shortest TS possible is selected when the best MF cannot be used. Using the same notation used for FLR-RA demonstration, after the definition of k transparent segments, the remaining part of the π not segmented yet is the same. However, the t_k depends on the MF used in the segment. If the best MF is used $t_k = x_k + 1$ because only one MF is checked. Otherwise, $t_k = Mx_k$ because, at most, all modulation formats are checked for all tested TSs and shortest TS is selected (in this case it is not necessary to TS-Check the next node and then come back if the TS- check fails). The second case is more time-consuming thus $t_k = Mx_k$. We can write then $\sum_{i=1}^{k} t_i = M \sum_{i=1}^{k} x_k$. Since $\sum_{i=1}^{k} x_k$ is, at most, $N-1$ then $\sum_{i=1}^{k} t_i$ is, at most, $M(N-1)$. It means that the FNS-RA algorithm needs at most $M(N-1)$ TS-Checks which leads to a $\mathcal{O}(M \cdot N)$ time complexity for FNS-RA.

The exhaustive algorithm needs to investigate all possibilities of using or not the renegerators in all possible regeneration points along a given route. Since there are $N-2$ regeneration points in π, there are 2^{N-2} possibilities of dividing the route in transparent segments. (for each regeneration point there are two options: either use or do not use the regenerators in that node). Each possibility found by the exhaustive algorithm segments the route into, at most, $N-1$ transparent segments. Each transparent segment requires, at most, one TS-Check for all M available modulation formats. Thus, in the worst case, the exhaustive algorithm performs $2^{N-2} \cdot (N-1) \cdot M$ TS-Checks which gives the time complexity of $\mathcal{O}(2^{N-2} \cdot M)$.

4 Simulation setup

In this section, we describe the scenarios and the most important considerations used in our simulations.

4.1 Dynamic traffic and call admission control

It is assumed a scenario of dynamic traffic in which call requests follow a Poisson process and the holding time of each established lightpath follows an Exponential distribution. The call requests are assumed unidirectional, and the source and destination nodes of each call request are randomly (uniform) selected. The slot bandwidth is 12.5 GHz and the transmission bit rate required by each demand is randomly (uniform) chosen among 100, 200 and 400 Gbps. Upon a call request, the call admission control (CAC) is triggered to find a route by using the shortest path algorithm. Then, the RA algorithm is applied to divide the route into transparent segments by using either FLR-RA, FNS-RA, Er-RA or Es-RA. After the transparent segments are defined, the first fit frequency spectrum assignment (FF-SA) is independently applied to each transparent segment. If RA does not return a solution, the call request is blocked, otherwise it is accepted and established. Note that an accepted call request must attend the QoT criterion, as well as frequency slot contiguity and continuity requirements in each transparent segment. The blocking probability is evaluated as the ratio of the number of blocked call requests to the number of all calls requested to the network. Two network physical topologies are investigated: (1) NSFnet (Topology 1), as shown in Fig. 1a [7], composed by 14 nodes and 21 bidirectional links (a pair of optical fibers in each direction), and (2) European (Topology 2), as shown in Fig. 1b [30], composed by 28 nodes and 41 bidirectional links. In the graphs shown in Sect. 5, the error bars for the 95% confidence interval are smaller than the graph symbols and for this reason they are not shown in the graphs. To obtain such result, each simulation point is simulated 30 times and the mean values are shown in the graphs. We have used in our simulations the simulation kernel from the SimEON simulator [31].

4.2 Physical layer

Each link in both network physical topologies is composed by several spans, in which the number of spans (s) is defined by the length of the link divided by the integer s that makes the span length as close as possible to 80 km. An erbium-doped fiber amplifier (EDFA) is deployed per span for signal amplification. The EDFA gain is set to compensate for link losses. Unless stated otherwise, it is assumed EDFA noise figure of 5.5 dB, a total of 320 available frequency slots per link, the modulation formats 4-QAM, 8-QAM and 16-QAM and transmitter signal power of 0.5 dBm for European and 0 dBm for NSFNet network physical topology.

Only the amplified spontaneous emission (ASE) noise is considered in the OSNR evaluation. Using this assumption, the accumulated noise is evaluated in this paper through the methodology proposed by Cavalcante et al. [32]. The required OSNR of each modulation format depends on the respective transmission bit rate of the call request and the desired BER after forward error correction (FEC). We have assumed a BER equal to 10^{-3}, which is a common value for hard-decision FECs. The required signal-to-noise ratio per bit (snr_b) may be defined for each modulation format. The relation between the required optical signal-to-noise ratio (osnr_{Th}) and snr_b is evaluated as in [33]. We have also assumed no dispersion compensation along the signal path,

whereas signal dispersion issues are compensated as currently assumed: using signal processing at the receiver [34].

We take into account the noise generated in the laser transmitter due to the spontaneous source emission (SSE) effect by considering the laser transmitter OSNR. The typical values for the laser OSNR are between 30 and 40 dB [35], and we have assumed the value of 40 dB in our simulations. The reason to select different transmitter optical powers for the two topologies is to enable that at least one of the assumed modulation formats is able to establish an all-optical lightpath from any source to any destination node in the network using the highest transmission bit rate. In order to investigate several different network conditions, we have also analyzed the scenarios with EDFA noise figure varying among the values 5 dB, 5.5 dB and 6.0 dB, several combinations of the following modulation formats: 4-QAM, 8-QAM, 16-QAM, 32-QAM and 64-QAM, different number of available frequency slots per link and transmitter optical launch powers of −2.0 dBm, −1.0 dBm and 0.0 dBm for NSFnet and −1.5 dBm, −0.5 dBm and 0.5 dBm for European network physical topology. Assuming the amplifier noise figure of 5.5 dB, launch powers of −2.0 dBm and −1.0 dBm (NSFnet) and −1.5 dBm and −0.5 dBm (European) results that at least one of the available transmission bit rates cannot be established without the use of regeneration resources in at least one source and destination pair. On the other hand, for the values of 0.0 dBm (NSFnet) and 0.5 dBm (European), all transmission bit rates and any source–destination pairs may be established using a single transparent segment (i.e., without regeneration points) under the most robust modulation format 4-QAM. The transmission reach for each modulation format, considering each given launching power, is evaluated using the same approach described in [9].

4.3 Node architecture and 3 R regenerators

It is assumed that all nodes are equipped with the node architecture known as spectrum switching [36] and a pool of R shared virtualized 3 R regenerators, as proposed in [37, 38]. The same number of regenerators are placed in all network nodes. It is assumed that the 3 R regenerators are capable to perform both modulation format and frequency spectrum conversion. Each of these regenerators has the capacity of regenerating bit streams of a specific transmission bit rate (b). It is possible to combine several regenerators in order to regenerate bit streams with higher transmission bit rates. For instance, if all regenerators at node A have $b = 100$ Gbps (as assumed in [7, 8, 21, 38] and in present paper as well), a call request of 100 Gbps requires one regenerator, whereas a call request of 400 Gbps requires 4 regenerators, and so on. Any lightpath may freely go through regeneration in a node if its required number of regenerators, as stated above, is free in that node.

5 Results

Figures 2 and 3 show the call request blocking probability as a function of the total number of regenerators installed in the NSFNet (European) network physical topology, Topology 1 (Topology 2), for a network load of 260 Erlang, considering: (a) 220, 270 and 320 frequency slots per link; (b) −2.0, −1.0 and 0.0 dBm (−1.5, −0.5 and 0.5 dBm) of transmitter launch power and (c) 5, 5.5 and 6 dB of EDFA noise figure. The FLR-RA (open symbol), FNS-RA (closed symbol), Er-RA (dashed line) and Es-RA (solid line) algorithms are simulated.

One can verify that, in both network physical topologies, even modifying several different physical and network layer parameters, the results found by FLR-RA and FNS-RA and

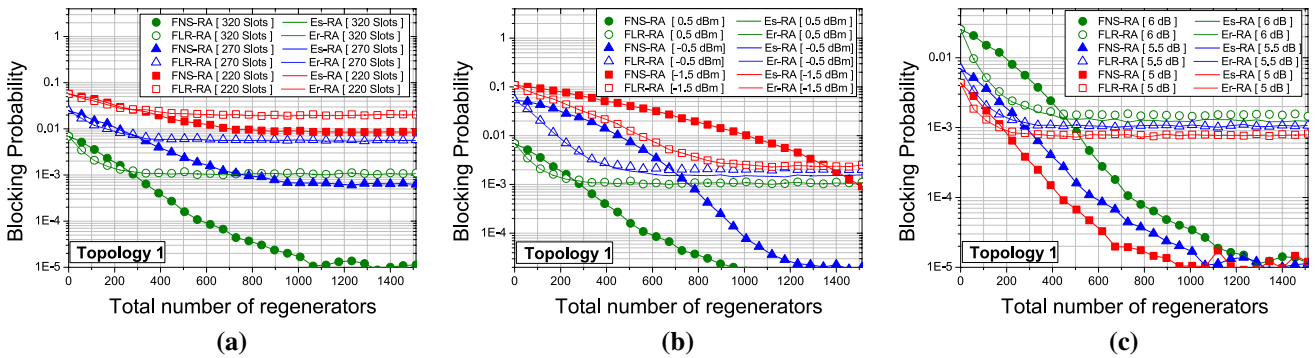

Fig. 2 Call request blocking probability as a function of the total number of regenerators installed in the NSFNet network physical topology, Topology 1, for a network load of 260 Erlang, considering: **a** 220, 270 and 320 frequency slots per link, **b** −2, −1 and 0 dBm of transmitter optical power and **c** 5, 5.5 and 6 dB of EDFA noise figure. The FLR-RA (open symbol), FNS-RA (closed symbol), Er-RA (dashed line) and Es-RA (solid line) algorithms were simulated to analyze their performances under distinct scenarios of both physical and network layers

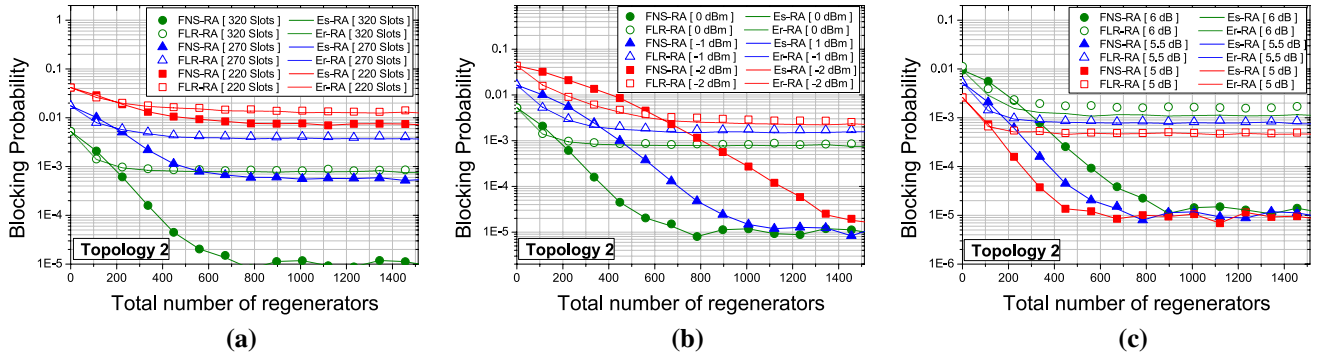

Fig. 3 Call request blocking probability as a function of the total number of regenerators installed in the European network physical topology, Topology 2, for a network load of 260 Erlang, considering: **a** 220, 270 and 320 frequency slots per link, **b** −1.5, −0.5 and 0.5 dBm of transmitter optical power and **c** 5, 5.5 and 6 dB of EDFA noise figure. The FLR-RA (open symbol), FNS-RA (closed symbol), Er-RA (dashed line) and Es-RA (solid line) algorithms were simulated to analyze their performances under distinct scenarios of both physical and network layers

their respective exhaustive counterparts are almost identical (compare lines and symbols with the same colors). It leads us to conclude that, in the analyzed scenarios, the proposed heuristics are able to find, for the majority of source–destination pairs, RA solutions that use the lowest possible number of their considered metric (either regenerators or frequency slots according to the case considered, i.e., FLR-RA or FNS-RA, respectively) and do not compromise the other metric. In other words, the heuristic algorithms are able to find very good solutions using significant lower computational complexity, as presented in Sect. 3.5.

In all investigated scenarios shown in Figs. 2 and 3, under a low number of regenerators installed in the respective network physical topologies, the call request blocking probability reduces with the increase in the number of regenerators. However, there is always a saturation point beyond which the addition of new regenerators results in no further reduction in the blocking probability. This occurs for all investigated RA algorithms. Although it is not possible to visualize the saturation level in the case for FNS-RA under −1.5 dBm, the trend of the plotted curve indicates that this threshold is achieved for a number of regenerators around 1500. The saturation level achieved by FNS-RA matches the lowest call request blocking probability that eventually could be reached with an equivalent opaque network. Notice the significant differences on blocking probability saturation levels between FLR-RA and FNS-RA in all investigated scenarios. The FNS-RA always saturates in lower values of blocking probabilities. It occurs due to its characteristics of using regeneration capabilities in exchange of spectrum savings, which is an efficient strategy under a large number of available regeneration resources.

By comparing the results found by FLR-RA and FNS-RA heuristics for any number of regenerators installed in the respective network physical topology, for each individual value of input parameter (i.e., comparing same shape, open against closed symbols) in Figs. 2 and 3, one may observe that there is always a crossing point between the curves. As expected and commented in Sect. 3, for low number of regenerators installed in the network physical topology, FLR-RA provides lower call request blocking probabilities than FNS-RA due to its regeneration saving aspect. On the other hand, for a large number of installed regenerators, an opposite result is obtained, since spectrum saving in such scenario favors FNS. As a conclusion, the selection of the suitable RA algorithm for the network depends on the number of regenerators installed per node. The crossing point as well as the blocking probabilities values found significantly varies according to the penalties imposed by the physical layer (transmitter optical power and EDFA noise figure) or network layer (number of available frequency slots).

Figures 4 and 5 shows the call request blocking probability, the average number of used regenerators and the average number of used frequency slots per established call as a function of network load for NSFNet (European) network physical topology, considering 4, 16 and 32 (4, 8 and 16) regenerators per node (each symbol/color stands for a given number of regenerators installed per node) using FLR-RA (open symbol), FNS-RA (closed symbol), Er-RA (dashed line) and Es-RA (solid line) algorithms.

Notice that, for a sufficiently low number of regenerators per node (ex. $R = 4$), FLR-RA finds lower call request blocking probabilities than FNS-RA for all analyzed network load. The opposite is verified for a sufficiently high number of regenerators. In the middle region of these two extremes, however, there might be a number of deployed regenerators such that the best RA algorithm depends on the network load itself. For instance, with 16 regenerators per node in Topology 1 (triangles in Fig. 4a), FNS-RA outperforms FLR-RA under low values of network

load, whereas FLR-RA outperforms FNS-RA under high network loads. A similar trend occurs in Topology 2, although the inversion occurs only for a high value of call request blocking probability.

The curves in Figs. 4 and 5 clearly demonstrate that FNS-RA tends to use, on average, more regeneration resources and less frequency slots per accepted request than FLR-RA (compare closed against open symbols in Figs. 4b, 5b and Figs. 4c, 5c). An interesting fact is that the heuristics have different trends regarding the regenerators usage: while FLR-RA increases the average use of regenerators per connection as the network load increases, FNS-RA shows an opposite trend (Figs. 4b, 5b). The trend of both heuristics is more similar regarding the average number of slots used per accepted request (Figs. 4c, 5c).

As the network load increases, the difficulty to satisfy the spectrum continuity constraint for the routes also increases. This condition forces FLR-RA to seek RA solutions that comply this restriction, which can be achieved by increasing the number of transparent segments in a route (and consequently the use of a larger number of regenerators). This explains the tendency of increasing the average number of regenerators per call verified by the FLR-RA results as the network load increases. Observe the open symbols curves in Figs. 4b and 5b to this conclusion. On the other hand, the increasing number of transparent segments reduces the physical length of each transparent segment. Smaller transparent segments enable the use of more efficient modulation formats, which explains the tendency of reduction in the average number of slots used per request by FLR-RA as the netwrok load increases, as shown by the open symbols curves in Figs. 4c and 5c.

A similar analysis can be performed to FNS-RA. The FNS-RA tries to reduce the size of transparent segments in order to use more efficient modulation formats. Thus, FNS-RA solutions naturally present many transparent segments. However, segmenting the path into larger transparent segments is also a valid solution that can be found by FNS, although in this case, a larger number of slots are eventually used. Therefore, the RA solution given by the

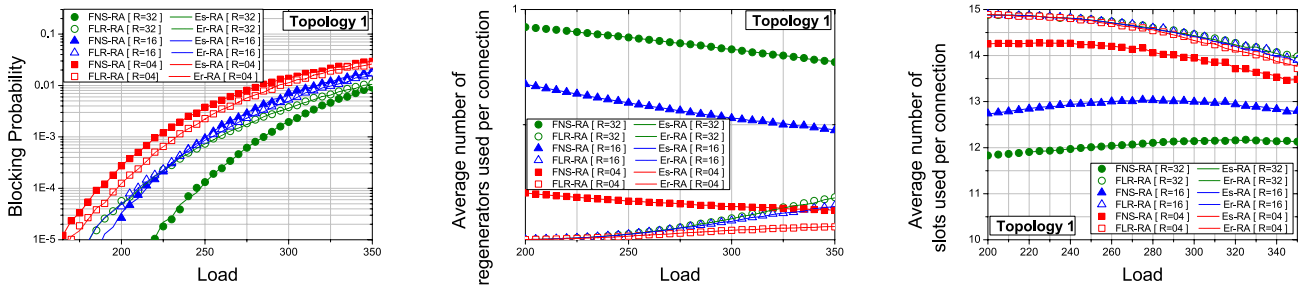

(a) Call request blocking probability. **(b)** Average number of used regenerators. **(c)** Average number of used frequency slots.

Fig. 4 **a** Call request blocking probability, **b** average number of used regenerators per established call request and **c** average number of used frequency slots per accepted request as a function of network load for NSFNet network physical topology, Topology 1, considering 4, 16 and 32 regenerators per node (each symbol/color stands for a given number of regenerators installed per node) for FLR-RA (open symbol), FNS-RA (closed symbol), Er-RA (dashed line) and Es-RA (solid line) algorithms

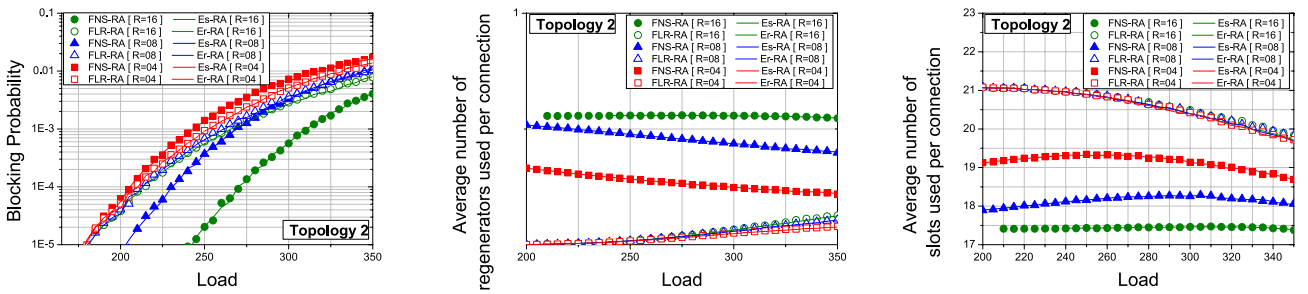

(a) Call request blocking probability. **(b)** Average number of used regenerators. **(c)** Average number of used frequency slots.

Fig. 5 **a** Call request blocking probability, **b** average number of used regenerators per established call request and **c** average number of used frequency slots per accepted request as a function of network load for European network physical topology, Topology 2, considering 4, 8 and 16 regenerators per node (each symbol/color stands for a given number of regenerators installed per node) for FLR-RA (open symbol), FNS-RA (closed symbol), Er-RA (dashed line) for Es-RA (solid line) algorithms

FNS-RA is strongly dependent on the number of regenerators available at the route nodes. As the network load increases, the availability of regenerators at the route nodes decreases on average. It forces FNS-RA to find solutions with longer transparent segments (which use fewer regenerators). This explains the tendency of the average number of regenerators to decrease as the network load increases. Observe curves in closed symbols in Figs. 4b and 5b for this conclusion. Longer transparent segments imply the use of less efficient modulation formats. This explains the slight tendency, at low load values, to increase the average number of slots as the load increases (curves in closed symbols in Figs. 4c, 5c). However, there is a certain load value beyond which the use of FNS-RA eventually exhausts the regeneration resources. The continuity constraint starts to impose blocking of several long routes (which are those that use more slots on average), which explains the reduction in slots usage as the load increases for high load values. Observe curves in closed symbols in Figs. 4c and 5c (the effect is more apparent when a small number of regenerators are deployed, as in the red curves in the graphs).

Figure 6 shows the call request blocking probability as a function of available number of frequency slots per link using 12 (square symbol), 40 (triangle symbol) and 56 (circle symbol) regenerators per node (each symbol/color stands for a given number of regenerators installed per node) under FLR-RA (open symbol), FNS-RA (closed symbol), Er-RA (dashed line) and Es-RA (solid line) algorithms applied to Topology 1 (Fig. 6a) and Topology 2 (Fig. 6b).

For a low number of regenerators (square symbol in Fig. 6), FLR-RA outperforms FNS-RA in the entire investigated range of available frequency slots, whereas, for a large number of regenerators (circle symbol in Fig. 6), an opposite behavior is observed. For an intermediary number of regenerators deployed (triangle symbol in Fig. 6), the best algorithm may depend on the number of frequency slots available in the network. Notice for Topology1 a performance inversion between FLR-RA and FNS-RA when around 260 frequency slots are assumed. Similar conclusion may be drawn analyzing the results for Topology 2 (as can be seen in Fig. 6b), except that a crossing point, as verified in Topology 1, has not been found for Topology 2 because a higher number of slots per link would be required.

The set of available modulation formats in the network directly affects the maximum optical reach without regeneration, which impacts the heuristics non-optimality conditions briefly discussed in Sect. 3.4. For this reason, we investigated scenarios using several different sets of available modulation formats in both network topologies. The results are shown in Fig. 7 (Topology 1) and in Fig 8 (Topology 2). These

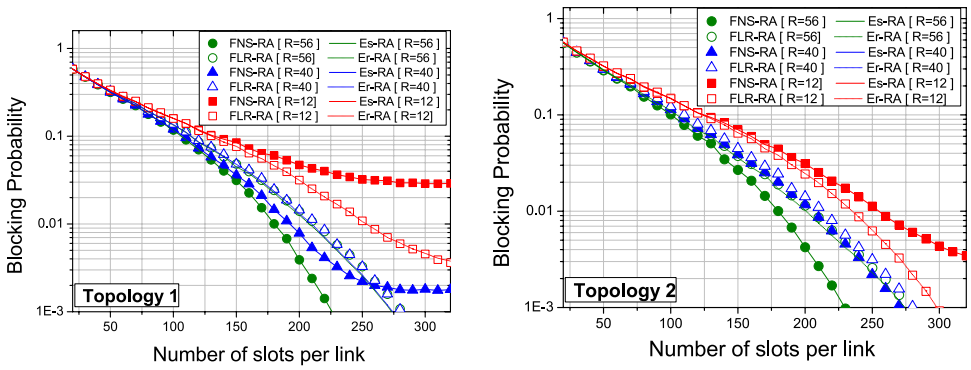

(a) Topology 1 **(b)** Topology 2

Fig. 6 Call request blocking probability as a function of available number of frequency slots per link using 12 (square symbol), 40 (triangle symbol) and 56 (circle symbol) regenerators per node (each symbol/color stands for a given number of regenerators installed per node) and FLR-RA (open symbol), FNS-RA (closed symbol), Er-RA (dashed line) and Es-RA (solid line) algorithms, considering: **a** Topology 1 and **b** Topology 2

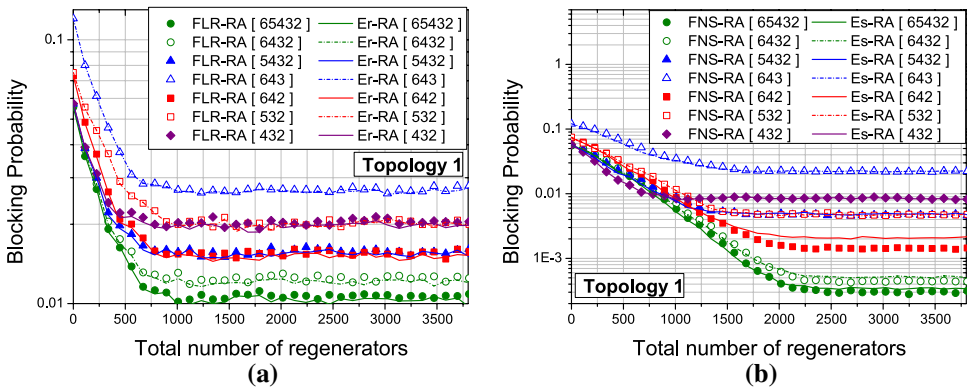

(a) **(b)**

Fig. 7 Call request blocking probability as a function of the number of regenerators installed in the network nodes for NSFNet (Topology 1), considering: **a** FLR-RA and Er-RA algorithms and **b** FNS-RA and Es-RA algorithms. The list of one digit integers $[n_1 n_2 \ldots n_i]$ inside the brackets in the figure caption represents the list of available QAM modulation formats: 2^{n_1}-QAM, 2^{n_2}-QAM,…,2^{n_i}-QAM

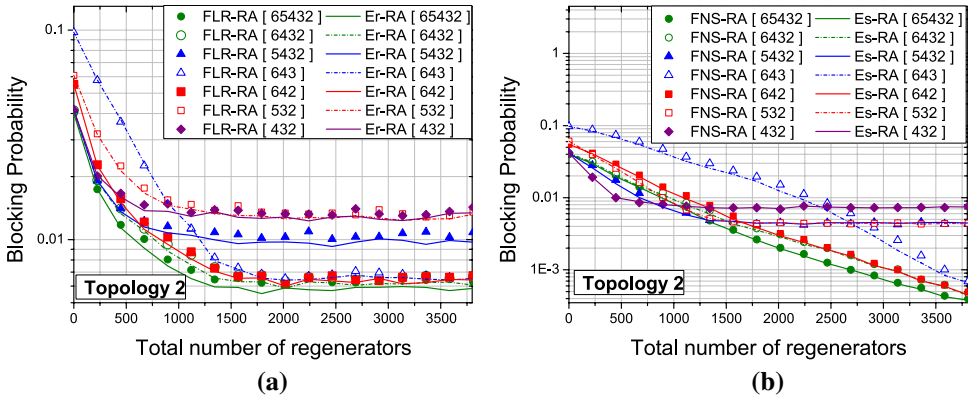

Fig. 8 Call request blocking probability as a function of the number of regenerators installed in the network nodes for European (Topology 2), considering: **a** FLR-RA and Er-RA algorithms and **b** FNS-RA and Es-RA algorithms. The list of one digit integers $[n_1 n_2 \ldots n_i]$ inside the brackets in the figure caption represents the list of available QAM modulation formats: 2^{n_1}-QAM, 2^{n_2}-QAM,…,2^{n_i}-QAM

results are obtained using 220 slots available per link. It is shown in these figures the call request blocking probability as a function of the number of regenerators installed in the network nodes for both topologies, considering: (a) FLR-RA and Er-RA algorithms and (b) FNS-RA and Es-RA algorithms. The number inside the brackets in the figure legend (n) stands for the set of available 2^n-QAM modulation formats. For instance, [432] stands for employing the following modulation formats: 2^4, 2^3 and 2^2-QAM, i.e., 16-QAM, 8-QAM and 4-QAM.

Different set of available modulation formats may generate situations in the network in which the results provided by FLR-RA and FNS-RA are non-optimum when compared to Er-RA and Es-RA, respectively. After analyzing several modulation format combinations, it is observed that FLR-RA and Er-RA, as well as FNS-RA and Es-Ra, usually obtain very similar results in terms of call request blocking probability. The greatest differences (although small) are observed only for the largest topology (topology 2) for the sets [65,432] and [5432] in Fig. 8a and [5432] in Fig. 8b. Note that, for a large number of regenerators deployed, the blocking probabilities found by FNS-RA are slightly lower than those found by Es-RA in some cases: [642], [65,432] and [6432] in Fig. 7b. The reason why this occurs is that FNS-RA may segment some routes in a grater number of TS than Es-RA. Thus, FNS-RA may achieve a slight improvement in spectrum packing on each TS. This facilitates the spectrum-continuity constraint fulfillment, which reduces blocking resultant from lack of spectrum continuity/contiguity.

Another interesting point to observe in Figs. 7 and 8 is that there are several crossover points between the blocking probabilities curves achieved by the use of different set of modulation formats. The crossover points are mainly observed in Figs. 7b, 8a, b. This implies that the availability of more modulation formats can even result in performance degradation. For instance, compare the curves achieved by using [65,432] (closed circles) against [432] (closed diamonds) in both topologies (Figs. 7b, 8b). For a low number of regenerators in the network, the use of the combination [432] (which uses three modulation formats) obtains lower blocking probability values than the combination [65,432] (which uses five modulation formats). This occurs because modulation formats with high spectral efficiency require the use of several regenerators in the network. Therefore, avoiding the use of such modulation formats forces regeneration savings. Such conclusion can be enforced on observing the high blocking probability of the set [643], i.e, when 4-QAM is removed. This occurs because 4-QAM is the one that can be transmitted further without regeneration. Therefore, its removal from the available modulation set incurs in high regeneration usage. On the other hand, the opposite is observed for a high number of regenerators, since the use of the combination [65,432] provides superior performance than [5432]. For a high number of regenerators, it is fundamental the inclusion of 64-QAM, since the sets [65,432], [6432], [643] and [642] are the ones with superior performance. This occurs because 64-QAM provides the highest spectral saving among the available modulation formats.

In all investigated scenarios so far, the heuristics and exhaustive algorithms showed very similar performance in terms of call request blocking probabilities. Thus, we have decided to investigate a scenario in which the non-optimality of the heuristics is guaranteed. We then use Eq. (1) to build this scenario. A simple network in which Eq. (1) assumptions (all links identical and with the same number of spans) are satisfied is a ring topology with identical link lengths. By setting EDFA noise figure to 5.5 dB, span length of 80 km, transmitter optical power of 0 dBm, and 8-, 16- and 64-QAM modulation formats available (i.e., $m = 3, 2, 1$ respectively), it is possible to find h_3, h_2, and h_1 (maximum optical signal reach) of approximately 34.52, 24.23 and 8.54 spans, respectively. These values are found by using the noise accumulated due to ASE noise and the OSNR thresholds for the considered modulation formats. As a result, Eq. (1) gives $8.6 < s < 11.5$ in such scenario. Thus, by selecting $s = 9$ spans per link, it is guaranteed the occurrences of heuristics

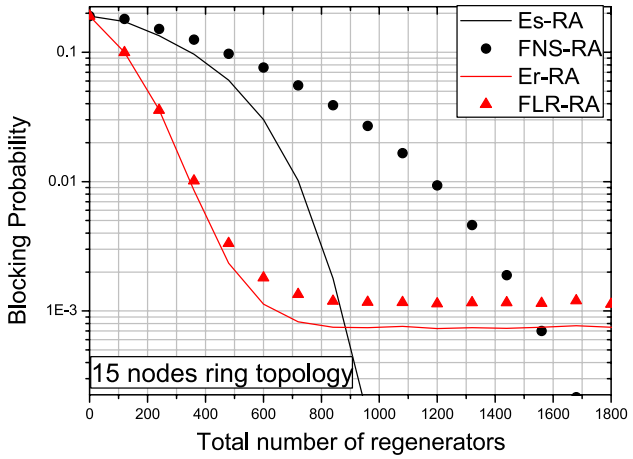

Fig. 9 Call request blocking probability as a function of the total number of regenerators using both heuristics (FLR-RA and FNS-RA) and exhaustive algorithms (Er-RA and Es-RA) in a 15 nodes ring physical network topology

non-optimal conditions for at least all 2- and 4-hop paths in the selected topology. Thus, it is simulated a 15-node ring topology with 9 spans of 80 km per link.

Figure 9 shows the call request blocking probability as a function of the total number of regenerators deployed in the 15-node ring topology obtained by FLR-RA and FNS-RA heuristics and their exhaustive counterparts Er-RA and Es-RA. Note that FLR-RA and Er-RA obtain almost the same values of blocking probabilities for a low number of regenerators deployed. However, as the number of installed regenerators increases, the Er-RA algorithm is able to find lower values of blocking probability, although the differences are not very pronounced. Similarly, FNS-RA and Es-RA obtain almost the same values of call request blocking probability for a low number of regenerators deployed. As the number of regenerators increases, however, Es-RA is able to find considerably lower values of call request blocking probability. We may conclude that, in some specific cases, the exhaustive algorithms may outperform their heuristics counterparts.

6 Conclusions

In this paper, we performed a detailed description and extensive performance analysis of two heuristics used to perform regenerator assignment in translucent EONs: FLR-RA and FNS-RA. The FLR-RA seeks to save the use of regenerators in the network, and FNS-RA seeks to save bandwidth by using regenerators to accomplish bandwidth savings. We have also compared the heuristics results against a recent exhaustive RA algorithm which provides a set of RA solutions that simultaneously among the optimum set determined by the exhaustive algorithm: Er-RA and Es-RA.

From the simulation analysis, we have concluded that the heuristics can achieve almost the same network performance levels, in terms of call request blocking probability, as the ones found by the exhaustive algorithms for typical mesh network scenarios. Thus, the heuristics may be applied to obtain near optimal solutions with the additional advantage of providing low computational complexity. The time complexity analysis performed in the algorithms states that the proposed heuristic algorithms show a linear time complexity, whereas the exhaustive algorithms' time complexities are exponential.

We also conclude that the best policy for regenerator assignment is strongly dependent on the network infrastructure, i.e., number of available frequency slots per link, number of regenerators available per node, optical parameters of physical layer devices, modulation formats available and network load to which the network is submitted. These factors together determine the best RA policy to be used on the network. The FNS-RA (FLR-RA) tends to present lower blocking probabilities than FLR-RA (FNS-RA) for high (low) network loads, low (high) number of available frequency slots per link and high (low) number of regenerators installed per node.

The blocking probability levels found by the investigated algorithms are also dependent on the set of available modulation formats. Moreover, in some cases, it was verified that using a smaller set of available modulation formats may result in lower values of blocking probability. This opens up room for optimization investigations regarding which would be the best set of modulation formats that should be used in the network as well as the possibility of installing less costly regenerators that would use a reduced set of modulation formats.

Acknowledgements The authors thank to CNPq and FACEPE for scholarships and grants, to UPE, UFCG and UFPE for their educational support.

References

1. Christodoulopoulos, K., Tomkos, I., Varvarigos, E.A.: Elastic bandwidth allocation in flexible OFDM-based optical networks. J. Lightwave Technol. **29**(9), 1354–1366 (2011)
2. Zhang, G., Leenheer, M.D., Morea, A., Mukherjee, B.: A survey on OFDM-based elastic core optical networking. IEEE Commun. Surv. Tutor. **15**(1), 65–87 (2013)
3. Chatterjee, B.C., Sarma, N., Oki, E.: Routing and spectrum allocation in elastic optical networks: a tutorial. IEEE Commun. Surv. Tutor. **17**(3), 1776–1800 (2015)
4. Yang, X., Ramamurthy, B.: Sparse regeneration in translucent wavelength-routed optical networks: architecture, network design and wavelength routing. Photonic Netw. Commun. **10**(1), 39–53 (2005)

5. Martins-Filho, J.F., de Santana, J.L., Pereira, H.A., Chaves, D.A.R., Bastos-Filho, C.J.A.: Assessment of the power series routing algorithm in translucent, transparent and opaque optical networks. IEEE Commun. Lett. **16**(6), 941–944 (2012)
6. Chaves, D.A.R., Carvalho, R.V.B., Pereira, H.A., Bastos-Filho, C.J.A., Martins-Filho, J.F.: Novel strategies for sparse regenerator placement in translucent optical networks. Photonic Netw. Commun. **24**(3), 237–251 (2012)
7. Chaves, D.A.R., da Silva, E.F., Bastos-Filho, C.J.A., Pereira, H.A., Almeida, R.C.: Heuristic algorithms for regenerator assignment in dynamic translucent elastic optical networks. In: International Conference on Transparent Optical Networks (ICTON), pp. 1–4 (2015)
8. Chaves, D.A.R., Cavalcante, M.A., Pereira, H.A., Almeida, R.C.: A case study of regenerator placement and regenerator assignment in dynamic translucent elastic optical networks. In: International Conference on Transparent Optical Networks (ICTON), pp. 1–4 (2016)
9. Cavalcante, M.A., Pereira, H.A., Chaves, D.A.R., Almeida, R.C.: Evolutionary multiobjective strategy for regenerator placement in elastic optical networks. IEEE Trans. Commun. **66**(8), 3583–3596 (2018)
10. Fallahpour, A., Beyranvand, H., Nezamalhosseini, S.A., Salehi, J.A.: Energy efficient routing and spectrum assignment with regenerator placement in elastic optical networks. J. Lightwave Technol. **32**(10), 2019–2027 (2014)
11. Willner, A.E., Fallahpour, A., Alishahi, F., Cao, Y., Mohajerin-Ariaei, A.H., Almaiman, A., Liao, P., Zou, K., Willner, A., Tur, M.: All-optical signal processing techniques for flexible networks. J. Lightwave Technol. **37**, 1621–1630 (2018)
12. Simmons, J.M.: Latency in verifying connection setup in dynamic optical networks. IEEE Netw. Lett. **1**, 1–4 (2018)
13. Jinno, M., Takagi, T., Uemura, Y.: Enhanced survivability of translucent elastic optical network employing shared protection with fallback. In: Optical Fiber Communications Conference and Exhibition (OFC), pp. 1–3 (2017)
14. Klinkowski, M., Walkowiak, K.: On performance gains of flexible regeneration and modulation conversion in translucent elastic optical networks with superchannel transmission. J. Lightwave Technol. **34**(23), 5485–5495 (2016)
15. Iyer, S.: Performance benefits of regeneration flexibility and modulation convertibility in elastic optical networks. Telecommun. Syst. **69**, 167 (2018)
16. Wang, X., Brandt-Pearce, M., Subramaniam, S.: Impact of wavelength and modulation conversion on translucent elastic optical networks using milp. IEEE/OSA J. Opt. Commun. Netw. **7**(7), 644–655 (2015)
17. Klinkowski, M., Walkowiak, K.: Performance analysis of flexible regeneration and modulation conversion in elastic optical networks. In: Optical Fiber Communications Conference and Exhibition (OFC), pp. 1–3 (2017)
18. Madani, F.M.: Scalable framework for translucent elastic optical network planning. J. Lightwave Technol. **34**(4), 1086–1097 (2016)
19. Dharmaweera, N., Yan, L., Zhao, J., Karlsson, M., Agrell, E.: Regenerator site selection in impairment-aware elastic optical networks. In: Optical Fiber Communications Conference and Exhibition (OFC), pp. 1–3 (2016)
20. Klinkowski, M.: On the effect of regenerator placement on spectrum usage in translucent elastic optical networks. In: International Conference on Transparent Optical Networks (ICTON), pp. 1–6 (2012)
21. Yamazaki, K., Matsushita, H., Jinno, M.: Virtualized-elastic-regenerator placement by firefly algorithm for translucent elastic optical networks. In: IEEE Congress on Evolutionary Computation (CEC), pp. 2866–2872 (2016)
22. Finochietto, J.M., Garrich, M., Bianco, A.: On provisioning strategies in translucent elastic optical networks with flexible regeneration and superchannel transmission. In: IEEE International Conference on High Performance Switching and Routing (HPSR), pp. 1–6 (2017)
23. Yan, L., Xu, Y., Brandt-Pearce, M., Dharmaweera, N., Agrell, E.: Robust regenerator allocation in nonlinear flexible-grid optical networks with time-varying data rates. IEEE/OSA J. Opt. Commun. Netw. **10**(11), 823–831 (2018)
24. Yang, S., Kuipers, F.: Impairment-aware routing in translucent spectrum-sliced elastic optical path networks. In: European Conference on Networks and Optical Communications, pp. 1–6 (2012)
25. Brasileiro, Í.B., Soares, A.C.B., dos Reis, J.V.: Planning and evaluation of translucent elastic optical networks in terms of cost-benefit. In: International Conference on Transparent Optical Networks (ICTON), pp. 1–4 (2017)
26. Guo, H., Li, Y., Li, L., Shen, G.: Adaptive modulation and regeneration-aware routing and spectrum assignment in sbpp-based elastic optical networks. IEEE Photonics J. **9**(2), 1–15 (2017)
27. Walkowiak, K., Klinkowski, M., Lechowicz, P.: Dynamic routing in spectrally spatially flexible optical networks with back-to-back regeneration. IEEE/OSA J. Opt. Commun. Netw. **10**(5), 523–534 (2018)
28. Gonzalez-Montoro, N., Finochietto, J.M., Bianco, A.: Optimal provisioning strategies for translucent elastic optical networks. In: 2018 IEEE Global Communications Conference (GLOBECOM), pp. 1–7 (2018)
29. Deb, K., Pratap, A., Agarwal, S., Meyarivan, T.: A fast and elitist multiobjective genetic algorithm: Nsga-II. IEEE Trans. Evol. Comput. **6**(2), 182–197 (2002)
30. Mello, D.A.A., Barreto, A.N., Lima, T.C., Portela, T.F., Beygi, L., Kahn, J.M.: Optical networking with variable-code-rate transceivers. J. Lightwave Technol. **32**(2), 257–266 (2014)
31. Cavalcante, M.A., Pereira, H.A., Almeida, R.C.: Simeon: an open-source elastic optical network simulator for academic and industrial purposes. Photonic Netw. Commun. **34**(2), 193–201 (2017). https://doi.org/10.1007/s11107-017-0697-9
32. Cavalcante, M.A., Pereira, H.A., Chaves, D.A.R., R.C.A. Jr., Applying power series routing algorithm in transparent elastic optical networks. In: SBMO/IEEE MTT-S International Microwave and Optoelectronics Conference (IMOC), pp. 1–5 (2015)
33. Essiambre, R.J., Kramer, G., Winzer, P.J., Foschini, G.J., Goebel, B.: Capacity limits of optical fiber networks. J. Lightwave Technol. **28**(4), 662–701 (2010)
34. Corsini, R., Peracchi, A., Matarazzo, E., Foggi, T., Nijhof, J., Meloni, G., Potì, L., Magri, R., Ciaramella, E.: Blind adaptive chromatic dispersion compensation and estimation for dsp-based coherent optical systems. J. Lightwave Technol. **31**(13), 2131–2139 (2013)
35. Fülöp, A., Mazur, M., Lorences-Riesgo, A., Helgason, Ó.B., Wang, P.-H., Xuan, Y., Leaird, D.E., Qi, M., Andrekson, P.A., Weiner, A.M., Torres-Company, V.: High-order coherent communications using mode-locked dark-pulse kerr combs from microresonators. Nat. Commun. **9**(1), 1598–1598 (2018)
36. Simeonidou, D., Amaya, N., Zervas, G.: Infrastructure and architectures on demand for flexible and elastic optical networks. In: European Conference and Exhibition on Optical Communications, pp. 1–3 (2012)
37. Jinno, M., Yonenaga, K., Takara, H., Shibahara, K., Yamanaka, S., Ono, T., Kawai, T., Tomizawa, M., Miyamoto, Y.: Demonstration of translucent elastic optical network based on virtualized elastic regenerator. In: OFC/NFOEC, pp. 1–3 (2012)
38. Jinno, M., Takara, H., Yonenaga, K., Hirano, A.: Virtualization in optical networks from network level to hardware level [invited]. IEEE/OSA J. Opt. Commun. Netw. **5**(10), A46–A56 (2013)

Emerson F. da Silva was born in Recife, Brazil, in 1985. He received the B.Sc (2011) degree in telecommunications Engineering and the M.Sc. degree in System Engineering from University of Pernambuco (UPE), Recife, Brazil, in 2016. His interests are related to Elastic Optical Networks (EON), regenerator placement (RP) and regenerator assignment (RA).

Raul C. Almeida Jr. has B.Sc. in Electronics Engineering from the Federal University of Pernambuco (1999) and M.Sc. (2001) and Ph.D. (2004) in Electrical Engineering from UNICAMP. Between 2006 and 2011, he has joined the University of Essex, UK, as a Senior Research Officer and in 2012 he joined the Photonics Group, Department of Electronics and Systems of UFPE, in Recife - Brazil, where is currently an Adjunct Professor. Raul C. Almeida Jr. has experience in Electrical Engineering, focusing on Telecommunication Systems, and his main interests are in optical networks, traffic engineering, analytical modeling, evolutionary computation, future Internet and telecommunication networks optimization and projects.

Helder A. Pereira was born in Paulista, Brazil, in 1980. He received the B.Sc. degree in Electronics Engineering from University of Pernambuco (UPE), Recife, Brazil, in 2000. The M.Sc. degree at Telecommunication National Institute (Inatel), Santa Rita do Sapucai, Brazil, in 2002. The Ph.D. degree in Electrical Engineering at the Federal University of Pernambuco (UFPE), Recife, Brazil, in 2007. He is a Professor at the Electrical Engineering Department of Federal University of Campina Grande (DEE-UFCG). His interests are related to fiber optics and optical communications, diffraction and gratings, optics and surfaces, medical optics and biotechnology.

Daniel A. R. Chaves was born in Recife, Brazil. He received the B.Sc (2006), M.Sc (2008) and Ph.D (2012) degrees in Electrical Engineering from Federal University of Pernambuco. He is a Professor of Computer Engineering at University of Pernambuco. Dr. Chaves is co-author of over 70 scientific papers related to optical networking, impairment aware RWA/RSA algorithms, design of all-optical and translucent networks and applications of computational intelligence in network optimization. Google Scholar: https://scholar.google.com/citations?user=fM6l2AMAAAAJ&hl=en, ResearcherID: F-7915-2011, orcid: 0000-0001-5274-6646